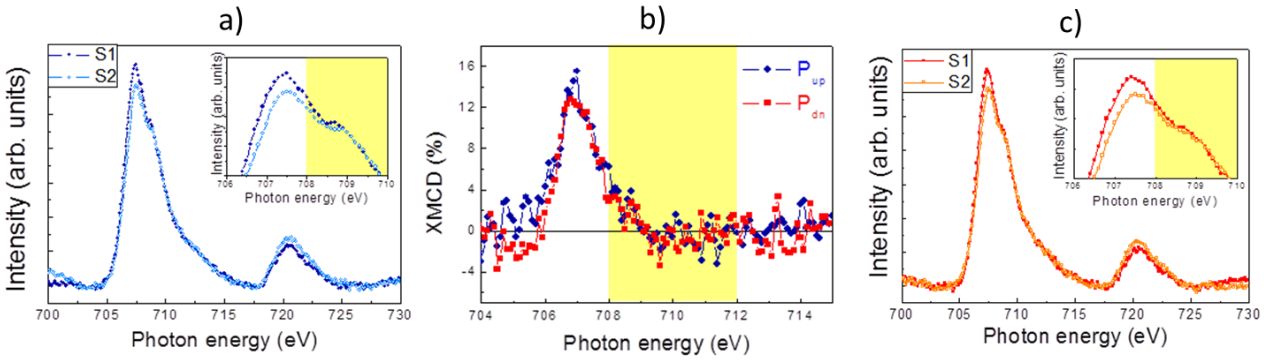

Supplementary Figure 1. Absence of XMCD after ferroelectric depolarization. (a) and (c) XAS Fe-$L_{2,3}$ spectra taken at room temperature on Au/Co/Fe(2ML)/BTO/LSMO//STO capacitors with A_1 = 0.02 mm^2 area after 30 min after polarization of BTO with V^+ = +5V (P_{up}) and V^- = -5V (P_{dn}) respectively. In the inset: zoom of the Fe-L_3 energy region. (b) XMCD signal in the Fe-L_3 energy region for BTO polarization P_{up} (blue circles) or P_{dn} (red squares).

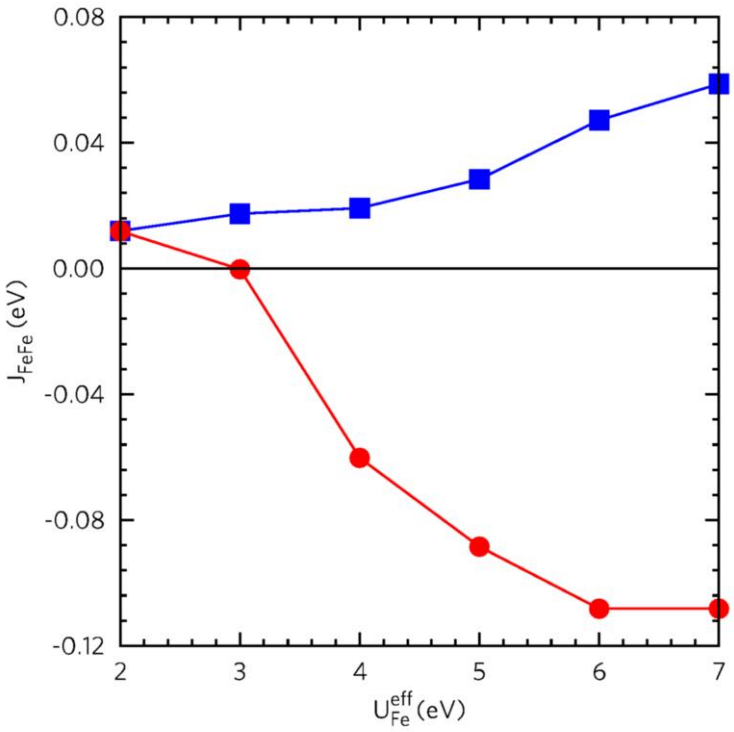

Supplementary Figure 2. **Exchange constants vs. *U* for 1 ML of Fe/BTO.** Exchange coupling constants (in eV) between Fe atoms of a single Fe ML, sandwiched between 1nm of Co and BTO, as a function of *U*. Blue squares represent the case of Interface I (P_{up}), whle red dots refer to Interface II (P_{dn}). For U > 3 eV the exchange constant becomes negative (AF coupling) only for Interface II.

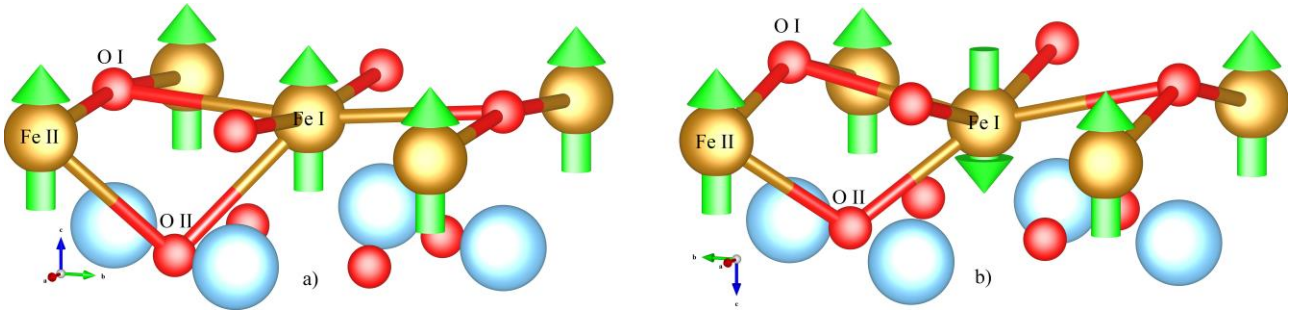

Supplementary Figure 3. Bond reconfiguration at the Fe/BTO interface. Details of the interface for the Ferromagnetic (a – Interface I) and Antiferromagnetic (b – Interface II) configurations of 1ML system. The FE polarization points in the direction of c-axis, upwards and downwards for the (a) and (b) configurations, respectively.

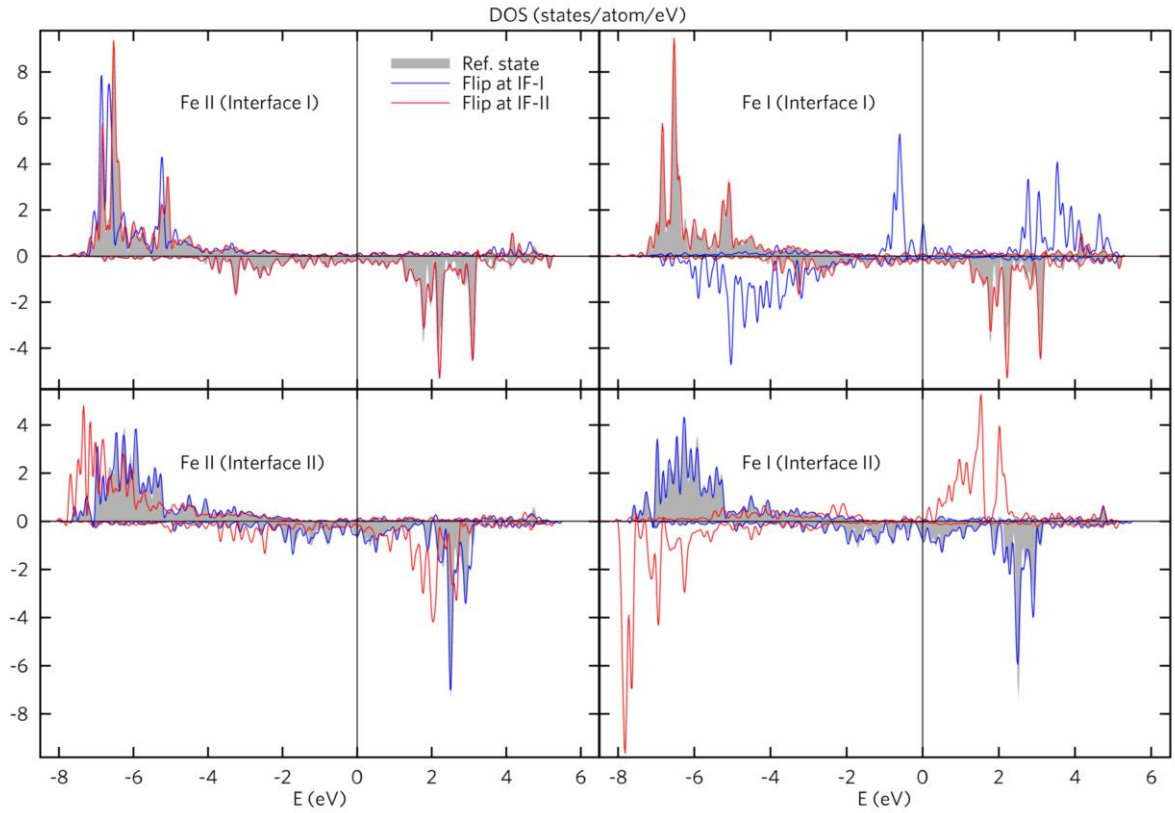

Supplementary Figure 4. Impact of the P direction on the electronic structure. Electronic structure for Co(9ML)/FeO(1ML)/BTO/FeO(1ML) supercell with PBC at U_{Fe}-J_{Fe}=5eV. Partial densities of states (PDOS) for two Fe atoms (Fe I and Fe II) at two different interfaces: Interface I (IF-I), corresponding to P_{up} (upper panels) and Interface II (IF-II), P_{dn}, (lower panels) in different spin configurations. The spin directions of the four Fe ions are reported in Supplementary Table 3.

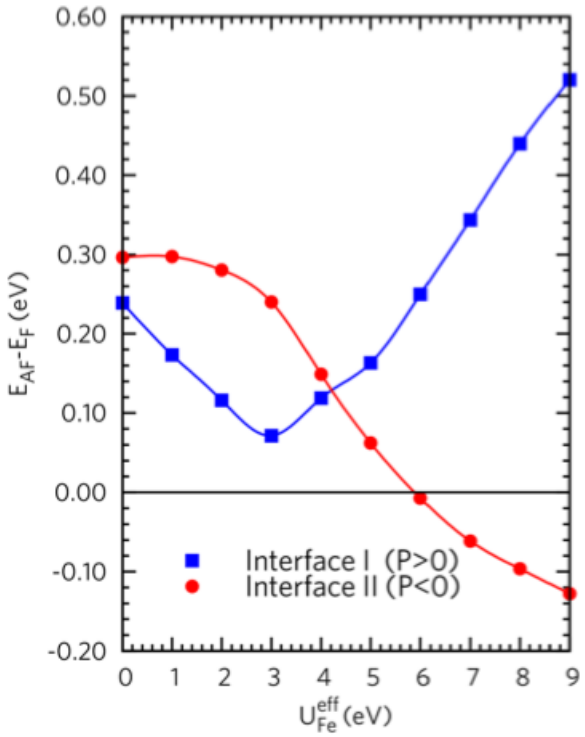

Supplementary Figure 5. Stability of FM and AF ordering vs. U in case of 2 ML of Fe. Energy difference between the AF and FM configuration for the case of 2ML of Fe on BTO (Co(9ML)/Fe(1ML)/FeO(1ML)/BTO/FeO(1ML)/Fe(1ML) with periodic boundary conditions). In good agreement with the results of the 1ML system, the switching to the AF state at large *U* is possible only at interface II, where the BTO polarization points downwards.

Co, Fe layers	flip #					
	0	1	2	3	4	5
Co N^{III}	↑↑	↓↓	↑↑	↑↑	↑↑	↑↑
Co N^{II}	↑↑	↑↑	↓↓	↑↑	↑↑	↑↑
Co NN	↑↑	↑↑	↑↑	↓↓	↑↑	↑↑
Fe	↑↑	↑↑	↑↑	↑↑	↓↓	↑↓

Supplementary Table 1. Spin configurations, as resulting from different spin flips, used for the evaluation of exchnage constants (see Supplementary Fig. 2 and Supplementary Note 2). Flip #0 represents the reference ferromagnetic state, while Co N^{III} denotes the Co layer at the third-neighbor out of plane distance with respect to the interface layer.

BTO polarization direction	Non-oxidized (meV)	Oxidized (meV)
P_{up}	43.54	11.96
P_{dn}	26.94	11.86

Supplementary Table 2. Estimation of the exchange energy term $J_{FeFe}S_{Fe}S_{Fe}$ (meV) for the two interface types. U_{Fe}-J_{Fe}=U_{Co}-J_{Co}=*2eV*.

	Interface I ($P_{\uparrow}$) (F)	Interface II ($P_{\downarrow}$) (AF)
Oxygen I, bond length Fe I-O I (Å)	2.83	2.90
Oxygen I, bond angle Fe I-O I-Fe II (º)	89.6	87.0
Oxygen II, bond length Fe I-O II (Å)	2.67	2.40
Oxygen II, bond angle Fe I-O II-Fe II (º)	96.7	112.3

Supplementary Table 3. Relevant structural details for 1ML of FeO/BTO. Bond angles and lengths from DFT calculations for the Co(10ML)/FeO(1ML)/BTO/FeO(1ML) system with PBC (see Supplementary Fig. 3).

	Interface I ($P_{\uparrow}$) (F)	Interface II ($P_{\downarrow}$) (AF)
Oxygen I, bond length Fe I-O I (Å)	2.84	3.06
Oxygen I, bond angle Fe I-O I-Fe II (º)	89.3	82.3
Oxygen II, bond length Fe I-O II (Å)	2.61	2.15
Oxygen II, bond angle Fe I-O II-Fe II (º)	99.8	133.3

Supplementary Table 4: Relevant structural details for 2ML case. Bond angles and lengths from DFT calculations for the Co(9ML)/Fe(1ML)/FeO(1ML)/BTO/FeO(1ML)/Fe(1ML) system with PBC.

	IF-I Fe I	IF-I Fe II	IF-II Fe I	IF-II Fe II
Ref. state (gray line)	↑	↑	↑	↑
Flip at IF-I (red line)	↓	↑	↑	↑
Flip at IF-II (blue line)	↑	↑	↓	↑

Supplementary Table 5: Spin directions of the four Fe ions for three different cases considered for the calculation of PDOS shown in Supplementary Fig. 4: i) Fe I spin-flip at interface I (IF-I), ii) Fe I spin flip at interface II (IF-II) and iii) the-ferromagnetic (non-flipped) configuration at both interfaces, denoted as Reference state.

Supplementary Note 1: XMCD showing that after depolarization there is no dichroism at the FeOx edge

In Supplementary Fig. 1 we show XAS and XMCD Fe-$L_{2,3}$ spectra taken at RT on the same sample of Fig. 5(a,b,c) in the main text (Au/Co/Fe(2ML)/BTO/LSMO//STO), but 30 minutes after BTO polarization, in order to allow BTO to depolarize. In particular, in panel (a) we show the XAS Fe-$L_{2,3}$ spectra taken long time after polarization of BTO with $V^+(P_{up})$. Spectra labelled S1 [S2] corresponds to the addition of spectra collected with (σ^+, m^+) and (σ^-, m^-) (= S1) [(σ^+, m^-) and (σ^-, m^+) (= S2)]. The prominent L_3 edge is formed by a main component at 707.4 eV, corresponding to metallic Fe^0, and a shoulder appearing at higher energy (~ 709 eV) and indicating some oxidized Fe^{m+} state. Focusing on L_3, where the intensity is higher and the background subtraction less critical, comparison of the S1 and S2 spectra, whose difference is the XMCD, shows the expected prominent dichroic signal at the Fe^0 edge at 707.4 eV, but no changes at the FeOx edge (~ 709 eV), as emphasized in Supplementary Fig. 1a (inset) and in Supplementary Fig. 1b, where we plot the XMCD signal in the energy region of interest (blue circles).

In Supplementary Fig. 1c we show the corresponding XAS Fe-$L_{2,3}$ spectra taken on the same sample long time (30 min) after polarization of BTO with V^- (P_{dn}). The large absorption of Fe^0 at ~ 707.4 eV and the FeOx signature ~ 709 eV can be readily observed; it is also clear that whereas a large difference between S1 and S2 spectra are observed at the Fe^0 edge, this difference disappear at the FeOx edge (~ 709 eV). This can be better appreciated in the zoom of the energy region of interest shown in Supplementary Fig. 1c (inset) and in Supplementary Fig. 1b, where we show the corresponding dichroic signal (red squares). A comparison of the XMCD signals of FeOx for P_{up} and P_{dn} (Supplementary Fig. 1b) clearly shows that the dichroic signal of FeOx is suppressed for both P_{dn} and P_{up} if we wait enough time before measuring, thus allowing BTO to depolarize.

It thus follows that the differences of XMCD between P_{up} and P_{dn} that we observe measuring after BTO polarization and that we have shown in Fig. 5 in the main text, become negligible when the samples are allowed to depolarize before XAS measurements. Note, however, that the reason why

the XMCD signal disappears after 30 minutes is most probably due to extrinsic effects related to the experimental set-up (spurious leakages and burden voltages). Indeed, the very same sample displayed remnant polarization even 1 hour after poling, if measured in a suitable apparatus for FE characterization via I-V measurements.

Supplementary Note 2: Details of the estimation of J_{FeFe} for 1 ML FeO/BTO

The estimation of magnetic exchange constants J_{FeFe} was done by mapping the total energies, calculated within Density Functional Theory (DFT), on a Heisenberg model, according to the following assumptions: i) Fe-Fe exchange was considered up to the in plane nearest neighbor (NN) distance; ii) Fe-Co and Co-Co exchanges were considered up to the out of plane next-NN (N^{II}) distance.

We have estimated J_{FeFe} for both a "non-oxidized" junction (i.e. Co/Fe/BaTiO3, where the interface Fe layer is similar to the structure simulated by Duan et al. [1] and the "oxidized" ($Co/FeO/BaTiO_3$) interface types, considering in both cases the $Fe/BaTiO_3$ interface capped with the Co layer. We recall that, in both oxidized and non-oxidized cases, there are two interface types, with polarization pointing towards and away from the $BaTiO_3$ layer (see Fig. 6a). Each interface contains two Fe atoms per plane; in the case of the oxidized interface originally containing only one Fe atom, the supercell has been doubled to allow for the AF ordering and for the estimate of the related exchange coupling. By flipping the spin on one of the two equivalent interface Fe atoms or on the Co atoms belonging to the neighboring Co layers, the supercell total energy changes. We denote these energy changes as $\Delta_i = E_i - E_0$ where i enumerates the flips in various Fe or Co layers and E_0 stands for the reference ferromagnetic state. It appears that under the above assumptions, five distinct flips need to be performed at each interface independently on the interface type. These flips are described in detail in Supplementary Table 1. Due to the difference in coordination between the two interface

types, these flips contribute to Δ_i in a different way. Namely, when mapping our DFT energy changes on a Heisenberg model for the magnetic energy term, the system of linear equations for the non-oxidized interface reads as follows:

$$\begin{aligned}
&32J_{CoCo}S_{Co}S_{Co} + 8J^2_{CoCo}S_{Co}S_{Co} = \Delta_1 \\
&32J_{CoCo}S_{Co}S_{Co} + 4J^2_{CoCo}S_{Co}S_{Co} + 4J^2_{FeCo}S_{Fe}S_{Co} = \Delta_2 \\
&16J_{CoCo}S_{Co}S_{Co} + 4J^2_{CoCo}S_{Co}S_{Co} + 16J_{FeCo}S_{Fe}S_{Co} = \Delta_3 \\
&16J_{FeCo}S_{Fe}S_{Co} + 4J^2_{FeCo}S_{Fe}S_{Co} = \Delta_4 \\
&8J_{FeFe}S_{Fe}S_{Fe} + 8J_{FeCo}S_{Fe}S_{Co} + 2J^2_{FeCo}S_{Fe}S_{Co} = \Delta_5
\end{aligned} \qquad (1)$$

On the other hand, the system of equations for the oxidized interface reads as follows:

$$\begin{aligned}
&64J_{CoCo}S_{Co}S_{Co} + 16J^2_{CoCo}S_{Co}S_{Co} = \Delta_1 \\
&64J_{CoCo}S_{Co}S_{Co} + 8J^2_{CoCo}S_{Co}S_{Co} + 4J^2_{FeCo}S_{Fe}S_{Co} = \Delta_2 \\
&32J_{CoCo}S_{Co}S_{Co} + 8J^2_{CoCo}S_{Co}S_{Co} + 16J_{FeCo}S_{Fe}S_{Co} = \Delta_3 \\
&16J_{FeCo}S_{Fe}S_{Co} + 4J^2_{FeCo}S_{Fe}S_{Co} = \Delta_4 \\
&8J_{FeFe}S_{Fe}S_{Fe} + 8J_{FeCo}S_{Fe}S_{Co} + 2J^2_{FeCo}S_{Fe}S_{Co} = \Delta_5
\end{aligned} \qquad (2)$$

We report in Supplementary Table 2 the exchange couplings estimated for the metallic (i.e. non-oxidized) and oxidized Fe layer at relatively small *U* values. Indeed, the comparison is meaningful only for small values of the Hubbard parameter, as correlation effects in metallic layers are presumably small (at variance with oxidized FeO layers where correlation effects can be much larger). The metallic interface presents, for both polarization directions, robust FM coupling. The latter are much larger than those estimated for the oxidized junction, where a strong competition between ferromagnetism and antiferromagnetism shows up (see Fig. 6 in the main text).

For the oxidized case, we compared the energy of the interface with ferromagnetically (F) and antiferromagnetically (AF) ordered Fe spins. As shown in Fig. 6b in the main text, at *U*~5eV the interface corresponding to the BTO polarization P_{dn} turns out to be antiferromagnetic, while the other interface (P_{up}) remains ferromagnetic. We found that this effect is enhanced by increasing *U* up to rather large values (*U* = 7 eV). Going back to our simulations for BTO/FeO/Co junctions, by mapping our DFT total energies to the simplified Heisenberg model described above, we estimated the exchange coupling constants J_{FeFe} for nearest neighbor Fe spins as function of *U*, as shown in

Supplementary Fig. 2. The U-dependence of J_{FeFe} reveals that the sign inversion of the exchange coupling occurs at even smaller U (~ 3 eV) and the difference between the two interfaces grows up even more upon increasing U. To interpret these results we note that the FeO interface is exposed to the strong local FM coupling induced by the ferromagnetic Co layer, which discourages the AF order. As a consequence, the AF configuration becomes energetically more stable at larger values of U: J_{FeFe} needs not only to be AF, but also large enough to overcome the "resistance" of the ferromagnetic Co side. This is possible only for P_{dn}, when the polarization induces a tangible change in the structure of FeO layer, with interfacial oxygen atoms jutting from the junction plane (cfr Fig. 6a and Supplementary Fig. 3). We emphasize that first-principles simulations, taking into account the complex junction geometry, are in this case mandatory to give an accurate description of the magnetic coupling; any simpler model based on Goodenough-Kanamori rules, crystal field effects, nominal valencies or comparison with bulk-FeO would be far too simplistic to describe our interface, which is constituted by one layer of FeO facing a strong FE on one side and a strong FM on the other side.

Supplementary Note 3: Polarization induced bond reconfiguration for 1 ML FeO/BTO

We here briefly discuss the relevant bond reconfiguration induced by polarization reversal in the case of 1ML of FeO. Supplementary Figure 3 shows the atomic arrangement at the FeO/BTO interface, as resulting from DFT calculations in case of the structure described in the main text: Co(9ML)/FeO(1ML)/BTO/FeO(1ML) with periodic boundary conditions (PBC). We note that there are two oxygen atoms that mediate the Fe-Fe interaction: the one in the FeO plane (O I) and the one in the TiO_2 plane (O II). Both of them are relevant, as the Fe-O bond lengths are comparable in the two cases (see Supplementary Table 3). As expected, we observe that the position of O II in the TiO_2 plane is more severely affected when switching polarization, in particular leading to a large increase in the Fe I-O II-Fe II angle (from 96.7 up to 112.3 degrees) at interface II (P_{dn}). Also the Fe I-O II bond length suffers from a sizable reduction upon polarization reversal (from 2.67 to 2.40 Å).

This clearly suggests that the O II atoms play a major role in the bond rearrangement leading to the switching of the magnetic order. Although the interface region is very complex and a simple model clearly cannot catch all the effects at play (this is also the reason why we opted for DFT calculations, which can take all the relevant effects into account on an equal footing), we can resort to the theory of super-exchange to provide a qualitative explanation of what we observe. Indeed, all Fe I-O-Fe II bonds connecting atoms whose coupling is switched from AFM to FM and vice versa, are 90° bonds, where exchange is very weak. Thus, this peculiar exchange interaction can be easily switched upon small perturbations (such as differences in the structural and electronic properties upon polarization switching), according to what we observe by XMCD.

Supplementary Note 4: Interplay between the AF-FM switching and the electronic structure for 1ML of FeO/BTO

Even though changes in the total energies (of the order of tens of meV per Fe atom) due to different spin-configurations are rather difficult to trace from the knowledge of the electronic structure, we here attempt to discuss changes in the electronic structure induced by either polarization switching (P_{up} vs P_{dn}) or switching in the magnetic ground state (FM vs AFM). Due to space limitations, we can't discuss the DOS of each atom for all *U* values; rather, we will concentrate on the electronic structure of the most relevant ions for a selected *U*. Recall that, in our unit cell, there are two different interfaces (IF-I with P_{up} and IF-II with P_{dn}), each containing two Fe atoms (Fe I at the center of the in-plane unit cell and Fe II at the corner of it). We show in Supplementary Fig. 4 the PDOS for the interface Fe ions in the two polarization states and in different magnetic configurations (for the different spin configuration of the Fe ions, see Supplementary Table 5) for an effective Hubbard-*U* of 5 eV. In general, we note that all Fe atoms show a fully occupied majority spin channel and a minority spin channel only partially occupied (by one electron, in a fully - and approximated - ionic picture). Fe II looks rather unchanged upon magnetic switching. On

the other hand, when concentrating on Fe I, whose spin direction was changed from "up" to "down", we observe that there is a larger exchange splitting in the AFM configuration, with occupied (unoccupied) minority (majority) states shifted at energies lower (higher) than in the corresponding up-spin state for Fe I (see Supplementary Fig. 4). In this situation, the shift of occupied states to lower energies leads to an energy gain in the sum-of-eigenvalues term of the DFT total energy: this is expected to contribute to the lowering of the energy in the AFM spin configuration. A similar but opposite argument can be invoked for Fe I in the down spin-state: the exchange splitting is smaller, therefore leading to an increase in the sum-of-eigenvalues-term, which justifies why interface I never stabilizes the AFM spin-configuration.

Supplementary Note 5: DFT calculation of the AF-FM switching for 2ML of Fe on BTO

In order to have a more comprehensive understanding of the effects of the oxidized Fe-layer and for additional comparison with experiments, we performed auxiliary calculations using 2ML of Fe (i.e. one monolayer of FeO and one additional Fe monolayer). The stack used for calculation was then: Co(9ML)/Fe(1ML)/FeO(1ML)/BTO/FeO(1ML)/Fe(1ML) with periodic boundary conditions. Even in this case we calculated the energy difference between the AF and FM spin configurations of the interfacial FeO layer depicted in the Supplementary Figure 3, for different values of the Hubbard energy *U*. The results are reported in the Supplementary Figure 5, showing a switching from FM to AF, occurring in the case of polarization pointing downwards at interface II. Therefore, although there are some qualitative changes with respect to the 1 ML case (the value of *U* at which the switching occurs is higher, and the energy differences between FM and AF spin configurations are lower), the physical picture is qualitatively unchanged, thus confirming the robustness of the mechanism proposed to explain the experimental magnetoelectric coupling. In the main manuscript the same mechanism was discussed with reference to the case of 1 ML FeO for two reasons: (i) it is much easier to treat from a computational point of view, and (ii) due to the island growth mode of

Fe on BTO (cfr. Fig. 2a in the main text) there are indeed some portions of the film with a FeO single ML coverage.

We also remark that the structural considerations presented above in the case of 1ML of Fe on BTO remain valid for the 2ML case. Indeed, when looking at the structural parameters reported in Supplementary Table 4 it is evident that a major bond reconfiguration involves the Fe I-O II-Fe II bond, between Fe atoms AF coupled through the oxygen atom of the TiO_2 plane underneath. This confirms that the mechanisms discussed above (Supplementary Note 3) for 1 ML are pertinent also to case of the nominal 2 ML Fe coverage used for XMCD experiments.

Supplementary Reference

[1] C-G. Duan, S. S. Jaswal and E. Y. Tsymbal, Predicted magnetoelectric effect in Fe/$BaTiO_3$ multilayers: Ferroelectric control of magnetism. *Phys. Rev. Lett*. **97**, 047201 (2006).